

Electronic Supplementary Information

Experimental section

Materials: Stannous chloride ($\text{SnCl}_2 \cdot 2\text{H}_2\text{O}$) was obtained from Chengdu jinshan Chemical Reagent Factory, China. Sodium nitroferricyanide dihydrate ($\text{C}_5\text{FeN}_6\text{Na}_2\text{O} \cdot 2\text{H}_2\text{O}$), salicylic acid ($\text{C}_7\text{H}_6\text{O}_3$), sodium citrate ($\text{Na}_3\text{C}_6\text{H}_5\text{O}_7 \cdot 2\text{H}_2\text{O}$), and para-(dimethylamino) benzaldehyde ($p\text{-C}_9\text{H}_{11}\text{NO}$) were purchased from Aladdin Ltd, Shanghai, China. Dipotassium hydrogen phosphate (K_2HPO_4) was purchased from Tianjin ruijinte chemical Co., Ltd. Ethyl alcohol ($\text{C}_2\text{H}_5\text{OH}$), Sulfuric acid (H_2SO_4), hydrochloric acid (HCl), sodium hydroxide (KOH), sodium borohydride (NaBH_4), 1, 10-phenanthroline ($\text{C}_{12}\text{H}_8\text{N}_2 \cdot \text{H}_2\text{O}$), tin (II) 2-ethylhexanoate ($\text{C}_{16}\text{H}_{30}\text{O}_4\text{Sn}$) and Potassium dihydrogen phosphate (KH_2PO_4) were bought from Chengdu Kelong Chemical Reagent Factory, China. Ammonium chloride (NH_4Cl), hypochlorite solution (NaClO), hydrazine monohydrate ($\text{N}_2\text{H}_4 \cdot \text{H}_2\text{O}$) and Sn foil (99.99%) were purchased from Beijing Chemical Corp, China. High-purity Ar (99.999%) and N_2 (99.999%) were purchased from Chengdu Xuyuan Chemical Co., Ltd, China. All reagents were analytical reagent grade without further purification. The ultrapure water used throughout all experiments was purified through a Millipore system.

Synthesis Sn dendrite on Sn foil (Sn D/SF): Sn dendrite is prepared by a simple electrodeposition method.¹ First, SF was polished with sandpaper and cleaned by deionized water and ethanol, last 0.1 M HCl. Then, 1 M HCl aqueous solution including 0.05 M SnCl_2 was prepared. In the three-electrode electrochemical system, Sn foil ($0.5 \times 1 \text{ cm}^2$) was used as working electrolysis, saturated calomel electrode (SCE) and Pt foil were used as reference electrode and counter electrode respectively. The Sn dendrite was synthesised by constant potential at -2.0 V (V vs. SCE) for 20 s. After deposition, The Sn dendrite was cleaned with deionized water and baked in an oven at 50°C for 1h.

Synthesis Sn nanoparticles (Sn NPs): In a typical synthesis process², 0.33 g of tin (II) 2-ethylhexanoate and 0.1 g of 1, 10-phenanthroline were mixed in 60 mL anhydrous methanol solution. The solution was then mechanically stirred intensively for 2 h. Then, 0.2 g of sodium borohydride was added to the solution and the reaction continued for another 2 h at room temperature. After the reaction completed, the obtained products were centrifugally separated at 8000 r/min for 30 min and rinsed several times with a large amount of absolute ethanol, and finally dried in vacuum at 60 °C for 4 h.

Preparation of Sn NPs/SF: 5 mg of Sn NPs and 20 μ L of Nafion solution (5 wt%) was dispersed in 980 μ L ethanol/water (1:1) solution followed by 20 min sonication to form a homogeneous ink. Finally, 30 μ L ink was loaded on a piece of SF (0.5 \times 1 cm²) and dried under ambient condition.

Characterization: X-ray diffraction (XRD) patterns were obtained from a Shimadzu XRD-6100 diffractometer with Cu K α radiation (40 kV, 30 mA) of wavelength 0.154 nm (Japan). Scanning electron microscopy (SEM) images were collected on a XL30 ESEM FEG scanning electron microscope at an accelerating voltage of 20 kV. The structures of the samples were determined by Transmission electron microscopy (TEM) images on a HITACHI H-8100 electron microscopy (Hitachi, Tokyo, Japan) operated at 200 kV. X-ray photoelectron spectroscopy graphs were obtained from a Thermo Scientific K-Alpha+. The absorbance data of spectrophotometer were measured on UV-Vis spectrophotometer.

Electrochemical measurement: Electrochemical NRR measurements were performed in a two-compartment cell separated by Nafion 117 membrane using a CHI 660E electrochemical analyzer (CHI Instruments, Inc., Shanghai). Nafion 117 membrane was ultrasonicated in 1 M H₂SO₄, and deionized water at 80 °C for 1 h, respectively. Then it was thoroughly rinsed in deionized water several times. The electrochemical experiments were carried out with a three-electrode H-type electrolytic cell using

graphite rod as the counter electrode and Ag/AgCl/saturated KCl as the reference electrode. The working electrode was Sn D/SF of $0.5 \times 1 \text{ cm}^2$ (Sn dendrite loading: 0.30 mg cm^{-2}) The potentials reported in this work were converted to reversible hydrogen electrode (RHE) scale via calibration with the following equation: $E(\text{RHE}) = E(\text{Ag}/\text{AgCl}) + 0.059 \times \text{pH} + 0.197 \text{ V}$ and the presented current density was normalized to the geometric surface area. Before all NRR test, Sn D/SF electrodes were pretreated by cyclic voltammograms (CVs) range from -0.24 to -0.60 V for cycling 30 times in Ar-saturated 0.1 M PBS electrolyte until the oxide layer reduction currents fully disappeared. The double layer capacitance is measured by cyclic voltammetry. A potential range from 0.4 to 0.5 V vs. RHE is chosen for the CV test under different scan rates of $20, 60, 100, 140, 180, 220 \text{ mV s}^{-1}$ without faradic current. The differences of positive and negative current density at the potential-range center were plotted vs. scan rates, the slope of curves were double capacitance. The chrono-amperometry tests were conducted in N_2 -saturated 0.1 M PBS solution (the PBS electrolyte was purged with N_2 for 30 min before the measurement).

Determination of NH_3 : Concentration of produced NH_3 was spectrophotometrically determined by the indophenol blue method.³ Typically, 2 mL electrolyte was taken from the cathodic chamber, and then 2 mL of 1 M NaOH solution containing 5% salicylic acid and 5% sodium citrate was added into this solution. Subsequently, 1 mL of 0.05 M NaClO and 0.2 mL of 1% $\text{C}_5\text{FeN}_6\text{Na}_2\text{O} \cdot 2\text{H}_2\text{O}$ were add into the above solution. After standing at room temperature for 2 h, UV-Vis absorption spectrum was measured at a wavelength of 655 nm . The concentration-absorbance curve was calibrated using the standard NH_4Cl solution with NH_3 concentrations of $0.0, 0.05, 0.10, 0.15, 0.20, 0.25,$ and $0.30 \mu\text{g mL}^{-1}$ in 0.1 M PBS. The fitting curve ($y = 0.364x + 0.057, R^2 = 0.999$) shows good linear relation of absorbance value with NH_3 concentration by three times independent calibrations.

Determination of N_2H_4 : N_2H_4 presented in the electrolyte was estimated by the method of Watt and Chrisp.⁴ The mixed solution of $5.99 \text{ g } p\text{-C}_9\text{H}_{11}\text{NO}$, 30 mL HCl and 300 mL ethanol was used as a color reagent. Calibration curve was plotted as

follow: firstly, preparing a series of reference solutions; secondly, adding 5 mL above prepared color reagent and stirring 20 min at room temperature; finally, the absorbance of the resulting solution was measured at 455 nm, and the yields of N_2H_4 were estimated from a standard curve using 5 mL residual electrolyte and 5 mL color reagent. Absolute calibration of this method was achieved using $N_2H_4 \cdot H_2O$ solutions of known concentration as standards, and the fitting curve shows good linear relation of absorbance with $N_2H_4 \cdot H_2O$ concentration ($y = 0.75x + 0.051$, $R^2 = 0.999$) by three times independent calibrations.

Calculations of NH_3 yield and Faradaic efficiency (FE): The FE for N_2 reduction was defined as the amount of electric charge used for synthesizing NH_3 divided the total charge passed through the electrodes during the electrolysis. The total amount of NH_3 produced was measured using colorimetric methods. Assuming three electrons were needed to produce one NH_3 molecule, the FE could be calculated as follows:

$$FE = 3 \times F \times [NH_3] \times V / (17 \times Q)$$

The rate of NH_3 yield (V_{NH_3}) was calculated using the following equation:

$$V_{NH_3} = [NH_3] \times V / (S_{cat.} \times t)$$

The amount of NH_3 was calculated as follows:

$$m_{NH_3} = [NH_3] \times V$$

Where F is the Faraday constant (96500 C mol^{-1}); $[NH_3]$ is the measured NH_3 concentration; V is the volume of the electrolyte in the cathodic chamber (35 ml); Q is the total quantity of applied electricity; $S_{cat.}$ is area of catalyst on Sn foil and t is the reduction time (7200 s).

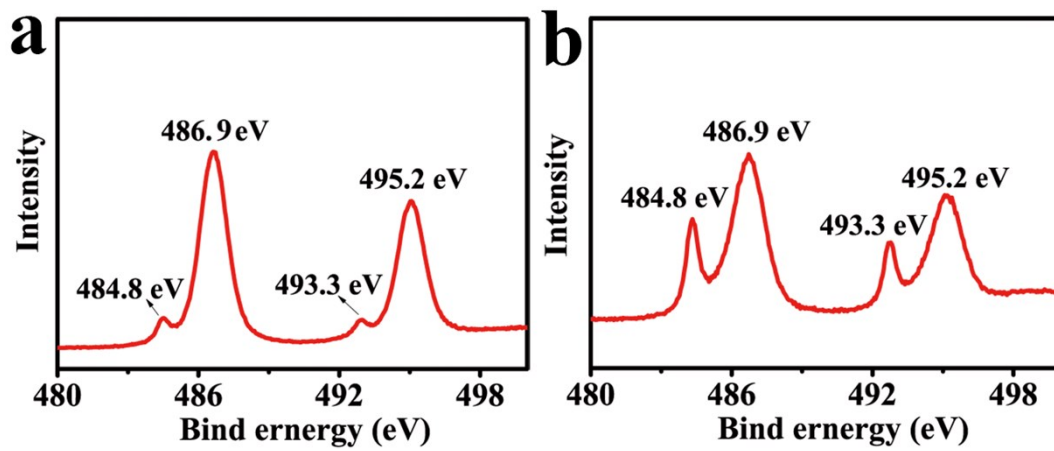


Fig. S1. XPS images of Sn dendrite: (a) Before test. (b) After test.

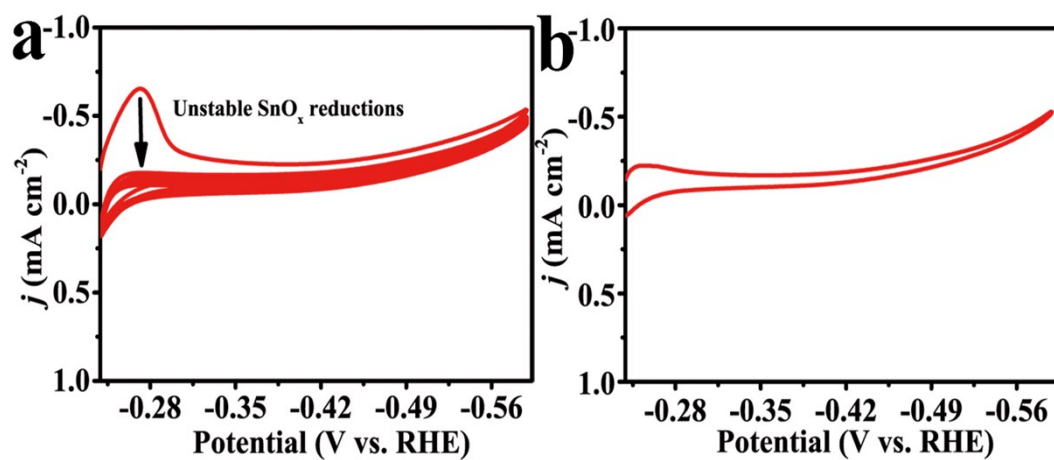


Fig. S2. (a) Stabilization of the Sn D/SF through cyclic voltammetry sweeping in Ar-bubbled 0.1 M PBS electrolyte. (b) CV of Sn D/SF after NRR test in Ar-bubbled 0.1 M PBS electrolyte.

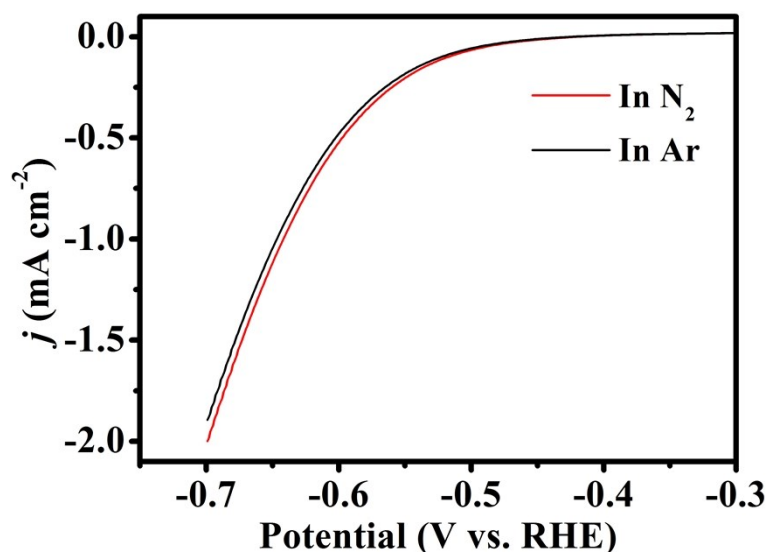


Fig. S3. LSV curves of Sn D/SF in Ar-saturated and N₂-saturated 0.1 M PBS with a scan rate of 5 mV s⁻¹.

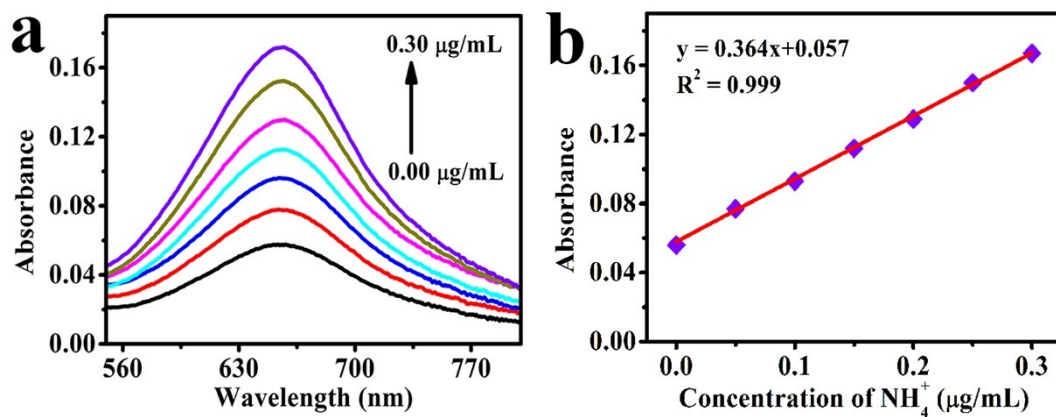


Fig. S4. (a) UV-Vis curves of indophenol assays with NH_3 after incubated for 2 h at room temperature. (b) Calibration curve used for estimation of NH_3 .

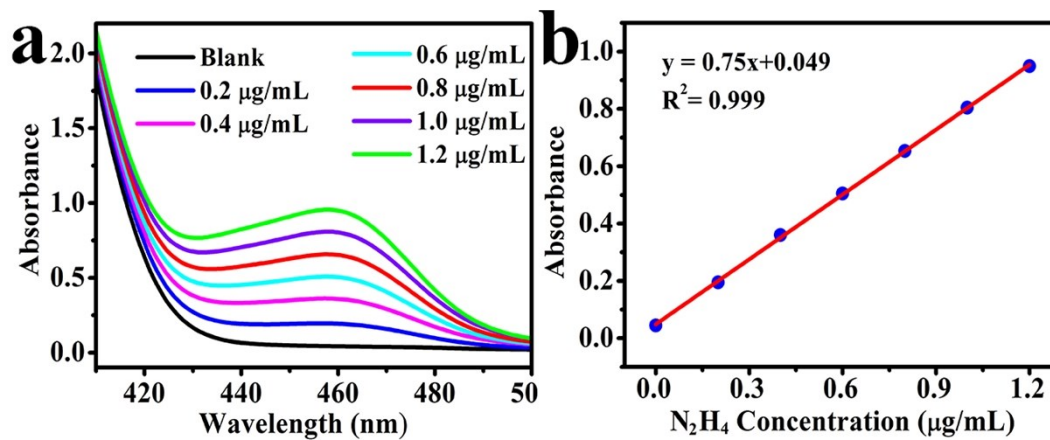


Fig. S5. (a) UV-Vis curves of various N_2H_4 concentrations after adding into chemical indicator by the method of Watt. (b) Calibration curve used for calculation of N_2H_4 concentrations.

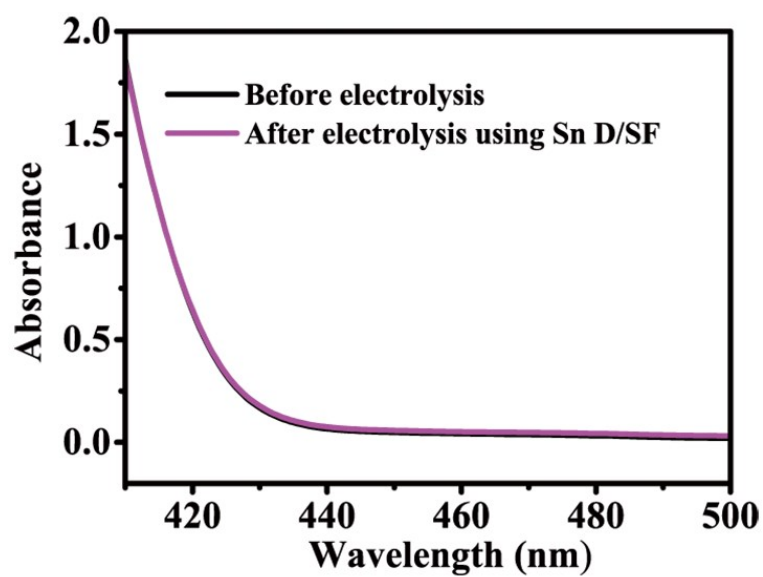


Fig. S6. UV-Vis absorption spectra of electrolytes stained with para-(dimethylamino) benzaldehyde indicator before and after 2 h electrolysis at -0.60 V.

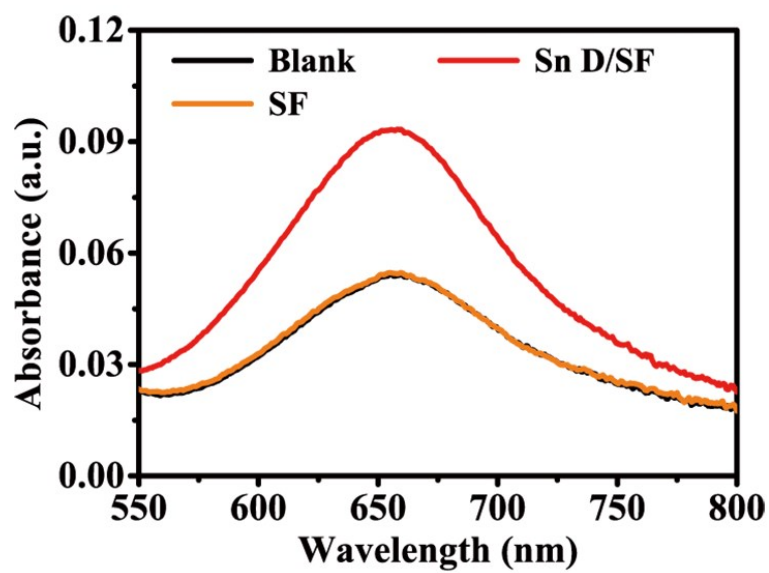


Fig. S7. UV-Vis absorption spectra of the electrolytes colored with indophenol indicator after 2 h electrolysis using different electrodes.

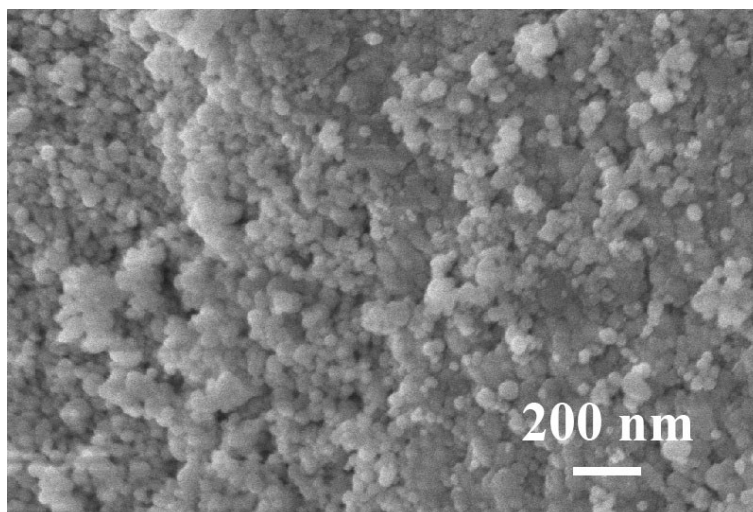


Fig. S8. SEM image of Sn nanoparticles

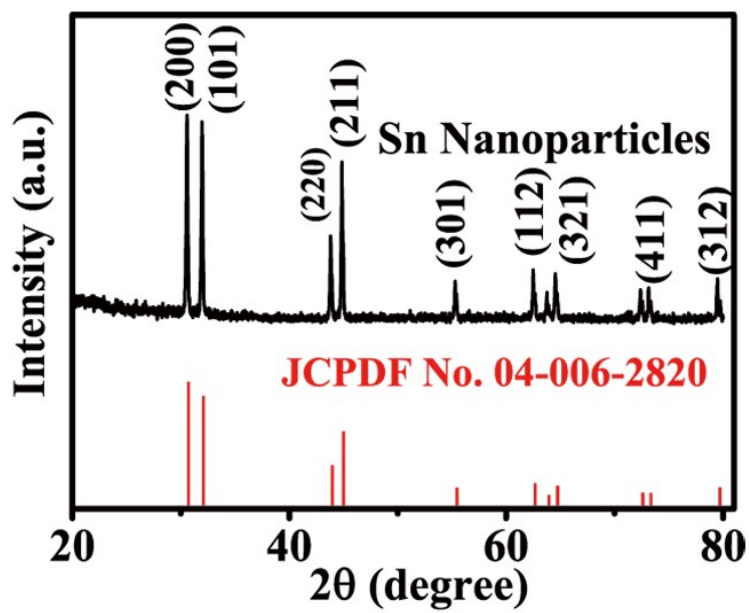


Fig. S9. XRD pattern of Sn nanoparticles

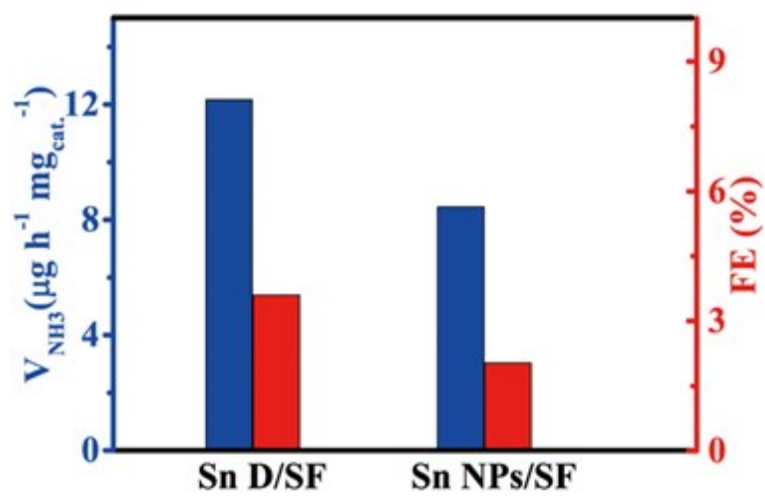


Fig. S10. NH_3 yields and FEs at -0.60 V for 2 h over Sn D/SF and Sn NPs/SF after 2-h testing.

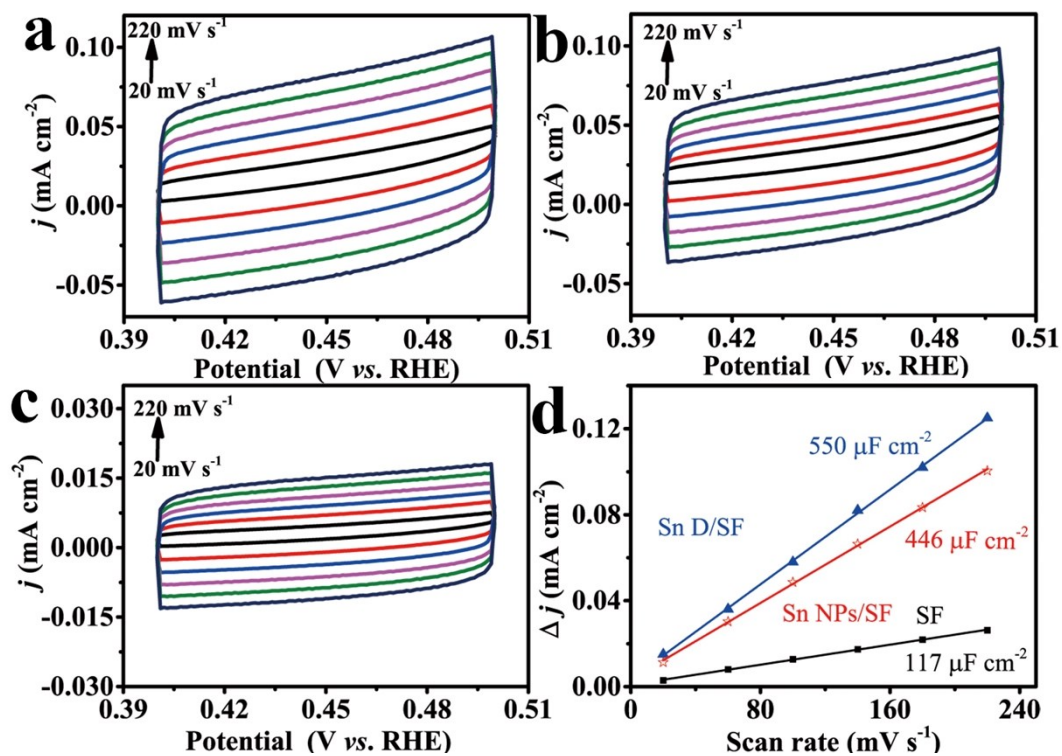


Fig. S11. CVs of (a) Sn D/SF, (b) Sn NPs/SF and (c) bare SF in the non-faradaic capacitance current range with various scan rates (20-220 mV s^{-1}) in the region of 0.40 to 0.50 V vs. RHE. (d) Corresponding capacitive currents at 0.45 V vs. RHE as a function of scan rates for Sn D/SF, Sn NPs/SF and SF.

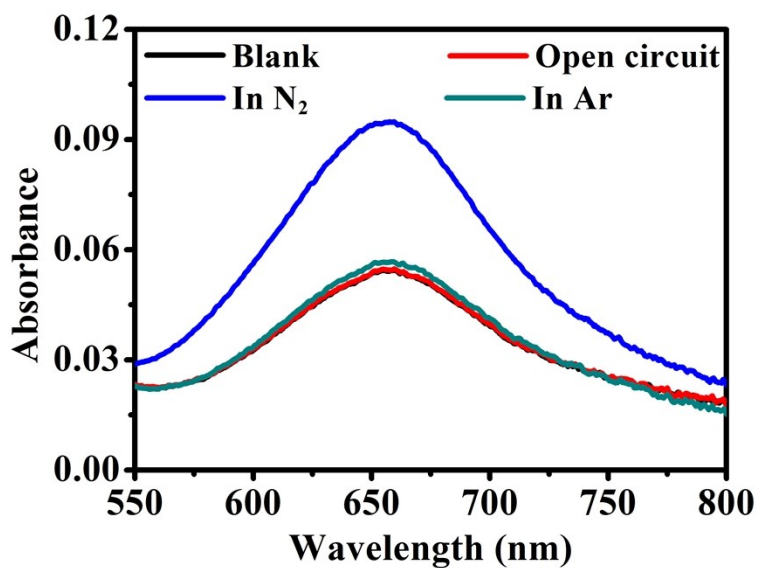


Fig. S12. UV-Vis absorption spectra of the electrolytes colored with indophenol indicator after 2 h electrolysis under different conditions.

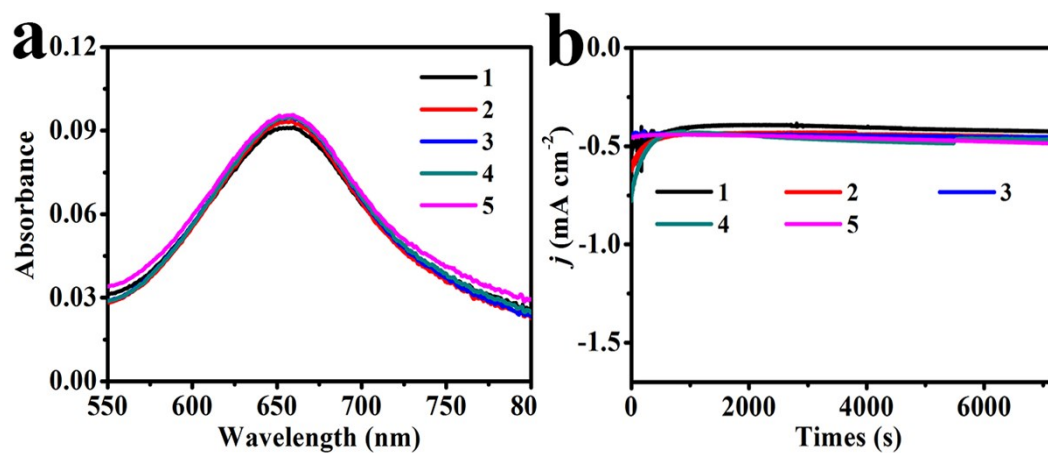


Fig. S13. (a) UV-Vis absorption spectra of the electrolytes stained with indophenol indicator after 2 h NRR electrolysis at -0.60V over 5 cycles. (b) Time-dependent current density curves of Sn/SF electrode at -0.60V for 5 cycles.

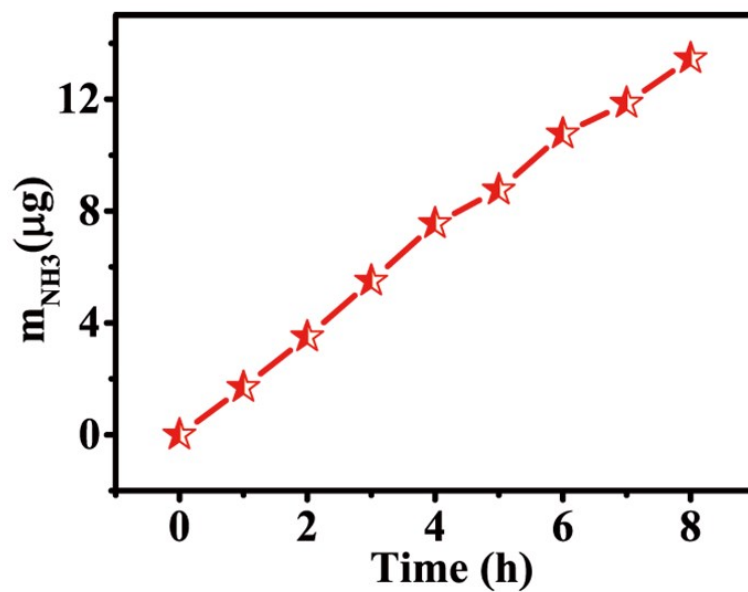


Fig. S14. m_{NH_3} vs. time recorded at -0.6 V in N_2 -saturated solution

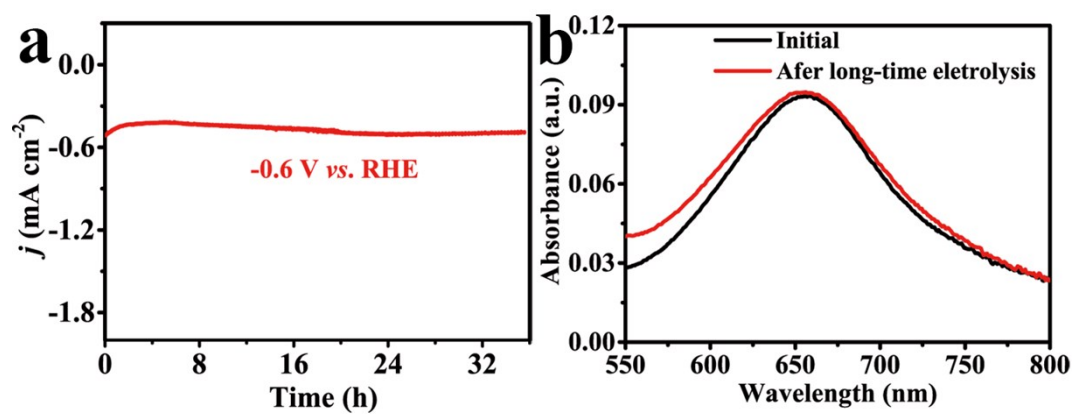


Fig. S15. (a) Time-dependent current density curve for Sn D/SF at -0.60 V for 36 h. (b) UV-Vis absorption spectra of the electrolytes stained with indophenol indicator at -0.60 V after electrolysis for 2 h with the initial and post-NRR electrolysis of Sn D/SF.

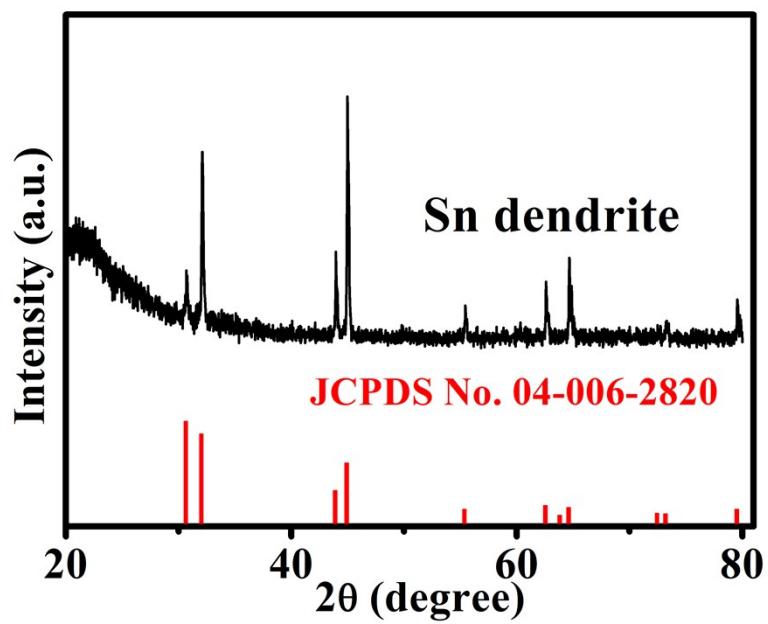


Fig. S16. XRD pattern of Sn dendrite scratched down from Sn foil after stability test.

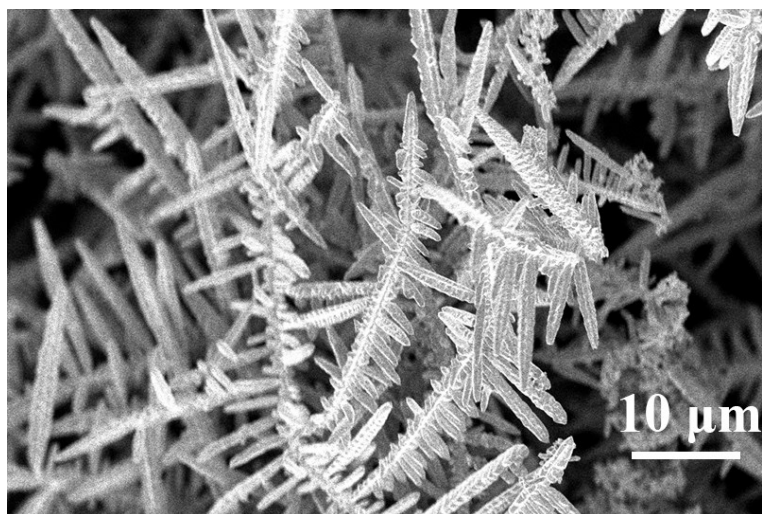


Fig. S17. SEM image of Sn D/SF after stability test.

Table S1. Comparison of the NH₃ yields and FEs for Sn/SF with other NRR electrocatalysts under ambient conditions.

Catalyst	Electrolyte	NH ₃ yield	FE (%)	Ref.
Sn D/SF	0.1 M PBS	$5.66 \times 10^{-11} \text{ mol s}^{-1} \text{ cm}^{-2}$	3.67	This work
		$12.17 \mu\text{g h}^{-1} \text{ mg}_{\text{cat}}^{-1}$		
SnO ₂	0.1 M Na ₂ SO ₄	$4.3 \mu\text{g h}^{-1} \text{ mg}_{\text{cat}}^{-1}$	2.17	5
F-SnO ₂ nanosheet	0.1 M Na ₂ SO ₄	$19.3 \mu\text{g h}^{-1} \text{ mg}_{\text{cat}}^{-1}$	8.6	6
SnO ₂ /rGO	0.1 M Na ₂ SO ₄	$25.6 \mu\text{g h}^{-1} \text{ mg}_{\text{cat}}^{-1}$	7.1	7
Fe ₂ O ₃ -CNT	0.1 M HCl	$3.58 \times 10^{-11} \text{ mol s}^{-1} \text{ cm}^{-2}$	0.15	8
Ru/C	2.0 M KOH	$3.44 \times 10^{-11} \text{ mol s}^{-1} \text{ cm}^{-2}$	0.28	9
Mo nanofilm	0.01 M H ₂ SO ₄	$3.09 \times 10^{-11} \text{ mol s}^{-1} \text{ cm}^{-2}$	0.72	10
Fe ₂ O ₃ nanorod	0.1 M Na ₂ SO ₄	$15.9 \mu\text{g h}^{-1} \text{ mg}^{-1}$	0.94	11
MoN nanosheets array	0.1 M HCl	$3.01 \times 10^{-10} \text{ mol s}^{-1} \text{ cm}^{-2}$	1.15	12
NPC	0.05 M H ₂ SO ₄	$1.40 \text{ mmol g}^{-1} \text{ h}^{-1}$	1.42	13
Fe ₃ O ₄ nanorod	0.1 M Na ₂ SO ₄	$5.6 \times 10^{-11} \text{ mol s}^{-1} \text{ cm}^{-2}$	2.6	14
PEBCD/C	0.5 M Li ₂ SO ₄	$2.01 \mu\text{g h}^{-1} \text{ cm}^{-2}$	2.85	15
Au nanorods	0.1 M KOH	$2.69 \times 10^{-11} \text{ mol s}^{-1} \text{ cm}^{-2}$	4.0	16
Ag nanosheet	0.1 M HCl	$4.62 \times 10^{-11} \text{ mol s}^{-1} \text{ cm}^{-2}$	4.8	17
Fe/Fe ₃ O ₄	0.1 M PBS	$0.19 \mu\text{g h}^{-1} \text{ cm}^{-2}$	8.29	18
NCM-Au NPs	0.1 M KOH	$0.36 \text{ g m}^{-2} \text{ h}^{-1}$	22	19
B nanosheet	0.1 M Na ₂ SO ₄	$13.22 \mu\text{g h}^{-1} \text{ mg}^{-1}$	4.04	20
W ₂ N ₃	0.05 M H ₂ SO ₄	$3.80 \times 10^{-11} \text{ mol s}^{-1} \text{ cm}^{-2}$	11.67	21
DyF ₃	0.1 M Na ₂ SO ₄	$10.9 \mu\text{g h}^{-1} \text{ mg}_{\text{cat}}^{-1}$	8.8	22
CoFe ₂ O ₄ /rGO	0.1 M Na ₂ SO ₄	$4.2 \times 10^{-11} \text{ mol s}^{-1} \text{ cm}^{-2}$	6.2	23
NiWO ₄	0.1 M Na ₂ SO ₄	$23.14 \mu\text{g h}^{-1} \text{ mg}_{\text{cat}}^{-1}$	10.18	24
NiCoS/C	0.1 M Li ₂ SO ₄	$26.0 \mu\text{g h}^{-1} \text{ mg}_{\text{cat}}^{-1}$	12.9	25

References

- 1 D. H. Won, C. H. Choi, J. Chung, M. W. Chung, E. H. Kim and S. I. Woo, *ChemSusChem.*, 2015, **8**, 3092–3098.
- 2 C. Zou, Y. Gao, B. Yang and Q. Zhai, *Trans. Nonferrous Met. Soc. China*, 2010, **20** 248–253.
- 3 Zhu, L. Zhang, R. E. Ruther and R. J. Hamers, *Nat. Mater.*, 2013, **12**, 836–841.
- 4 G. W. Watt and J. D. Chrisp, *Anal. Chem.*, 1952, **24**, 2006–2008.
- 5 L. Zhang, X. Ren, Y. Luo, X. Shi, A. M. Asiri, T. Li and X. Sun, *Chem. Commun.*, 2018, **54**, 12966–12969.
- 6 Y. Liu, Y. Li, H. Zhang and K. Chu, *Inorg. Chem.*, 2019, **58**, 10424–10431.
- 7 K. Chu, Y. Liu, Y. Li, J. Wang and H. Zhang, *ACS Appl. Mater. Interfaces*, 2019, **11**, 31806–31815.
- 8 S. Chen, S. Perathoner, C. Ampelli, C. Mebrahtu, D. Su and G. Centi, *Angew. Chem., Int. Ed.*, 2017, **56**, 2699–2703.
- 9 V. Kordali, G. Kyriacou and C. Lambrou, *Chem. Commun.*, 2000, **17**, 1673–1674.
- 10 D. Yang, T. Chen and Z. Wang, *J. Mater. Chem. A*, 2017, **5**, 18967–18971.
- 11 X. Xiang, Z. Wang, X. Shi, M. Fan and X. Sun, *ChemCatChem.*, 2018, **10**, 4530–4535.
- 12 L. Zhang, X. Ji, X. Ren, Y. Luo, X. Shi, A. M. Asiri, B. Zheng and X. Sun, *ACS Sustainable Chem. Eng.*, 2018, **6**, 9550–9554.
- 13 X. Yang, K. Li, D. Cheng, W. Pang, J. Lv, X. Chen, H. Zang, X. Wu, H. Tan, Y. Wang and Y. Li, *J. Mater. Chem. A*, 2018, **6**, 7762–7769.
- 14 Q. Liu, X. Zhang, B. Zhang, Y. Luo, G. Cui, F. Xie and X. Sun, *Nanoscale.*, 2018, **10**, 14386–14389.
- 15 G. Chen, X. Cao, S. Wu, X. Zeng, L. Ding, M. Zhu and H. Wang, *J. Am. Chem. Soc.*, 2017, **139**, 9771–9774.

- 16 D. Bao, Q. Zhang, F. Meng, H. Zhong, M. Shi, Y. Zhang, J. Yan, Q. Jiang and X. Zhang, *Adv. Mater.*, 2017, **29**, 1604799.
- 17 H. Huang, L. Xia, X. Shi, A. M. Asiri and X. Sun, *Chem. Commun.*, 2018, **54**, 11427–11430.
- 18 L. Hu, A. Khaniya, J. Wang, G. Chen, W. E. Kaden and X. Feng, *ACS Catal.*, 2018, **8**, 9312–9319.
- 19 H. Wang, L. Wang, Q. Wang, S. Ye, W. Sun, Y. Shao, Z. Jiang, Q. Qiao, Y. Zhu and P. Song, *Angew. Chem., Int. Ed.*, 2018, **57**, 12360–12364.
- 20 X. Zhang, T. Wu, H. Wang, R. Zhao, H. Chen, T. Wang, P. Wei, Y. Luo, Y. Zhang and X. Sun, *ACS Catal.*, 2019, **9**, 4609–4615.
- 21 H. Jin, L. Li, X. Liu, C. Tang, W. Xu, S. Chen, L. Song, Y. Zheng and S. Qiao, *Adv. Mater.*, 2019, **31**, 1902709.
- 22 Y. Li, T. Li, X. Zhu, A. A. Alshehri, K. A. Alzahrani, S. Lu and X. Sun, *Chem. Asian J.*, 2020, **15**, 487–489.
- 23 M. I. Ahmed, S. Chen, W. Ren, X. Chen and C. Zhao, *Chem. Commun.*, 2019, **55**, 12184–12187.
- 24 J. Wang, H. Jang, G. Li, M. G. Kim, Z. Wu, X. Liu and J. Cho, *Nanoscale* 2020, **12**, 1478–1483
- 25 X. Wu, Z. Wang, Y. Han, D. Zhang, M. Wang, H. Li, H. Zhao, Y. Pan, J. Lai and L. Wang, *J. Mater. Chem. A*, 2020, **8**, 543–547.